JOURNAL OF THE AMERICAN CHEMICAL SOCIETY

Communication

Diastereomer Assignment of an Olefin-Linked Bis-paracyclophane by Ion Mobility Mass Spectrometry

Erin Shammel Baker, Janice W. Hong, Jennifer Gidden, Glenn P. Bartholomew, Guillermo C. Bazan, and Michael T. Bowers

J. Am. Chem. Soc., **2004**, 126 (20), 6255-6257• DOI: 10.1021/ja039486k • Publication Date (Web): 01 May 2004

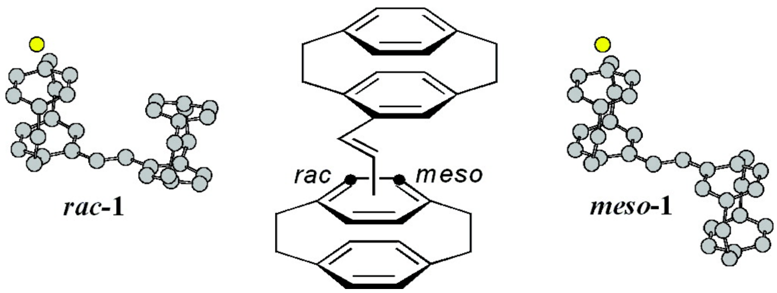

J|A|C|S
COMMUNICATIONS

Published on Web 05/01/2004

Diastereomer Assignment of an Olefin-Linked Bis-paracyclophane by Ion Mobility Mass Spectrometry

Erin Shammel Baker,[†] Janice W. Hong,[†,‡] Jennifer Gidden,[†] Glenn P. Bartholomew,[†,‡] Guillermo C. Bazan,*[,†,‡] and Michael T. Bowers*[,†]

Department of Chemistry and Biochemistry, and Department of Materials, Center for Polymers and Organic Solids, University of California, Santa Barbara, California 93106

Received November 7, 2003; E-mail: bazan@chem.ucsb.edu; bowers@chem.ucsb.edu

Stereochemistry relates to the three-dimensional arrangement of atoms in molecules and is a fundamental chemical concept.[1] A wide range of biological functions and physical properties are determined by molecular recognition and complementarity, which implicitly requires stereochemical information. In view of this importance, methods for the determination of absolute spatial relationships in organic diastereomers have been of remarkable historical significance.[2]

Interest in examining how the [2.2]paracyclophane (pCp) core influences electronic coupling between organic chromophores[3] led us to consider *trans*-1,2-bis([2.2]paracyclophanyl)ethene (**1**), which holds a pair of pCp cores together by an olefinic linkage. As shown in Figure 1, two diastereomers, meso ((*S*,*R*), *meso*-**1**)[4] or racemic ((*R*,*R*) or (*S*,*S*), *rac*-**1**; only (*R*,*R*)-**1** is shown), are possible, corresponding to the chirality of the olefin−pCp plane.[5] In this contribution, we provide synthetic entries into the two diastereomers of **1** and describe an approach for the determination of diastereomer identity.

As shown in Scheme 1, we sought entry into **1** by olefin metathesis coupling of *rac*-4-vinyl[2.2]paracyclophane catalyzed by (PCy_3)(1,3-dimesityl-4,5-dihydroimdazol-2-ylidene)methylidene $RuCl_2$ [PCy_3 = tricycloheyxlphosphine] (Scheme 1 (i)).[6] NMR spectroscopy, mass spectrometry, and HPLC analysis indicated that this synthetic route yielded primarily one product (>95%). However, differentiation between the *meso*-**1** and *rac*-**1** forms was not possible using NMR spectroscopy, and efforts to obtain a single crystal suitable for X-ray diffraction studies failed, because the product yields small polycrystalline “beads”.

An alternative synthesis was by Heck reaction[7] of *rac*-4-vinyl-[2.2]paracyclophane with *rac*-4-bromo[2.2]paracyclophane using $Pd(OAc)_2$ (Scheme 1 (ii)). In this case, ^1H NMR spectroscopy and HPLC analysis indicated that the product was ∼30% of the same diastereomer as from the olefin metathesis reaction and ∼70% of a second form.

Information about the olefinic linkage connectivity was obtained using ion mobility experiments and molecular mechanics calculations. In the ion mobility experiments,[8,9] sodiated ions of **1**, formed by MALDI, are mass selected and injected at low energy into a drift cell[10] containing ∼1.5 Torr of He. The ions are rapidly thermalized by collisions with the He gas and travel through the drift cell under the influence of a weak electric field (7.5−16 V/cm). Ions exiting the drift cell are collected as a function of time, yielding an arrival time distribution (ATD). Because the drift time of the ions is directly proportional to their collision cross section,[11] the ion size can be determined. Compact ions with small collision cross sections drift faster and have shorter arrival times than more extended ions with larger cross sections. Thus, different conformers can be separated in the drift cell and will appear as separate peaks in the ATD if their cross sections differ by at least 4%,[12] and they do not interconvert as they drift.[13,14]

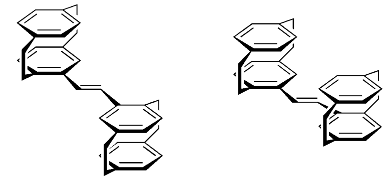

meso-**1** *racemic*-**1**

Figure 1. The structure of *meso*-**1** and *racemic*-**1**.

Scheme 1 [a]

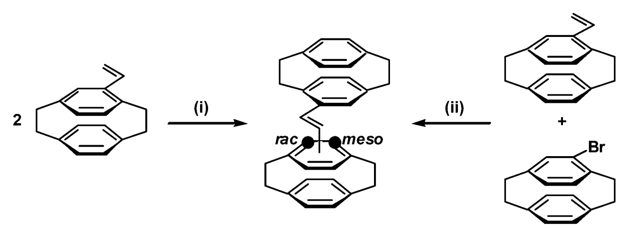

1

[a] (i) (PCy_3)(1,3-dimesityl-4,5-dihydroimidazol-2-ylidene)methylidene $RuCl_2$, CH_2Cl_2, 45 °C, overnight. (ii) $Pd(OAc)_2$, $P(o\text{-}tol)_3$, $N(Et)_3$, DMF, 70 °C, 36 h.

Racemic and meso connectivity details for sodiated-**1** were obtained by comparing the experimental ATD cross sections to the collision cross sections of theoretical structures. For calculations, a series of annealing and energy minimizations using AMBER 6.0 programs[15] were used to generate 100 low-energy structures for both the sodiated meso (Na^+*meso*-**1**) and the racemic (Na^+*rac*-**1**) forms. A temperature-dependent model[12,16] with appropriate atomic collision radii calculated from the ion−He interaction potential was used to calculate the angle-averaged collision cross sections for each theoretical structure. A scatter plot of cross sections versus energies for both Na^+*rac*-**1** and Na^+*meso*-**1** was then used to identify the lowest energy family of structures.

Figure 2 illustrates the ATDs for sodiated-**1** ions obtained from (a) olefin metathesis and (b) Heck reactions. A single ion peak is observed in Figure 2a with a collision cross section of 137 ± 2 Å^2. Figure 2b shows two peaks, corresponding to collision cross sections of 138 ± 2 and 144 ± 2 Å^2. The distribution of products determined by the ATDs is consistent with the NMR spectroscopy and HPLC results.

Theoretical modeling of *meso*-**1** and *rac*-**1** provides very different conformations. Representations of the lowest energy family of structures for each diastereomer are shown in Figure 3.

In Na^+*meso*-**1**, the pCp cores are positioned in an “up/down”, steplike configuration with one pCp above the plane of the olefinic

[†] Department of Chemistry and Biochemistry.
[‡] Department of Materials.

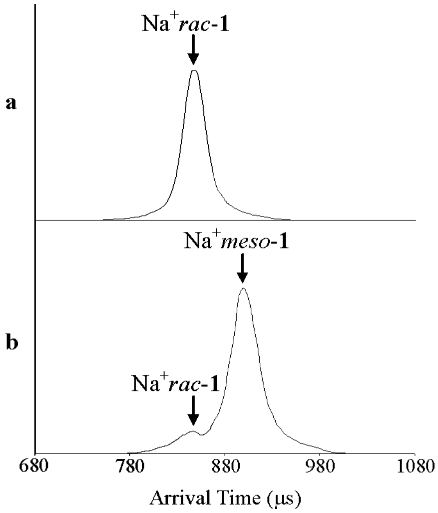

Figure 2. Arrival time distributions of Na$^+$ olefin-linked pCp ions taken at 300 K for (a) reaction i in Scheme 1 and (b) reaction ii in Scheme 1. The arrows indicate theoretically predicted arrival times for Na$^+$*meso*-**1** and Na$^+$*rac*-**1**.

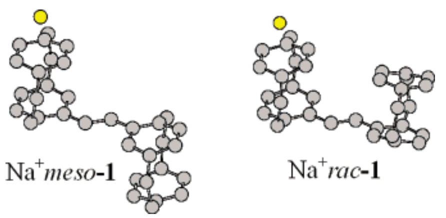

Figure 3. Calculated low-energy structures of Na$^+$*meso*-**1** and Na$^+$*rac*-**1**. Carbon atoms are gray, and sodium atoms are yellow. Hydrogen atoms are omitted for clarity.

Table 1. Experimental and Theoretical Cross Sections

isomer	cross sections (Å^2) experiment	cross sections (Å^2) theory
Na$^+$*rac*-**1**[a]	137 ± 2	139 ± 2
Na$^+$*meso*-**1**[a]	144 ± 2	144 ± 2
Na$^+$(*R*,*S*,*S*,*S*)-**2**[b]	139 ± 2	140 ± 2
Na$^+$(*R*,*R*,*R*,*R*)-**2**[b]	140 ± 2	140 ± 2
Na$^+$(*R*,*S*,*S*,*R*)-**2**[b]	145 ± 2	145 ± 2

[a] Olefinic-linked structures in Figure 1. [b] Epoxide-linked structures in Figure 5.

linkage and the other pCp below the plane. The Na$^+$ ion "binds" to one pCp face, but essentially acts as a spectator ion without forcing a particular conformation. The calculated average cross section of Na$^+$*meso*-**1** is 144 ± 2 Å^2, in excellent agreement with the experimental value obtained for the longest time peak from the Heck reaction (see Table 1). In Na$^+$*rac*-**1**, the Na$^+$ also attaches to one face of the pCp unit, but the overall molecule adopts a distorted "up/up" configuration with an average cross section of 139 ± 2 Å^2. This value is in excellent agreement with the experimental cross section obtained for the shortest time peak from the Heck reaction and the only peak for the olefin metathesis reaction. Thus, the correlation between calculated and experimental ATD values allows one to determine that olefin metathesis provides *rac*-**1** with greater than 95% selectivity, while the Heck reaction preferentially yields *meso*-**1**.

To compare against traditional chemical diastereomer assignment methods,[1] a reviewer suggested olefin epoxidation (Scheme 2). The products from *meso*-**1** are the enantiomeric pair (*R*,*S*,*S*,*S*)-**2** and (*R*,*R*,*R*,*S*)-**2**, which should have identical ATDs. Epoxidation of *rac*-**1** from the more hindered face gives rise to (*R*,*S*,*S*,*R*)-**2** and

Scheme 2[a]

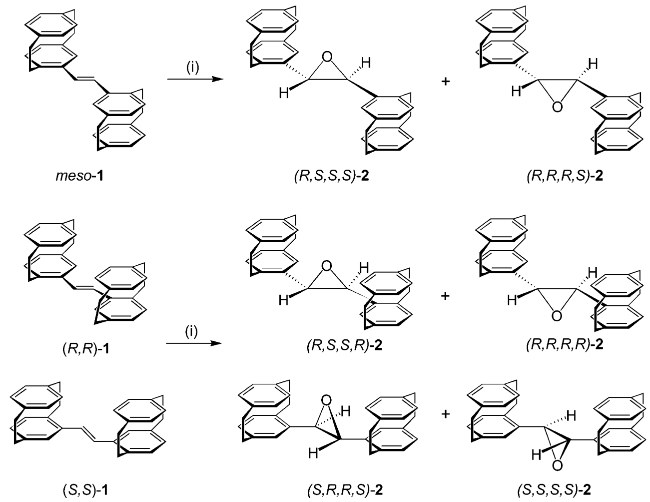

[a] (i) MCPBA, CH_2Cl_2, 25 °C.

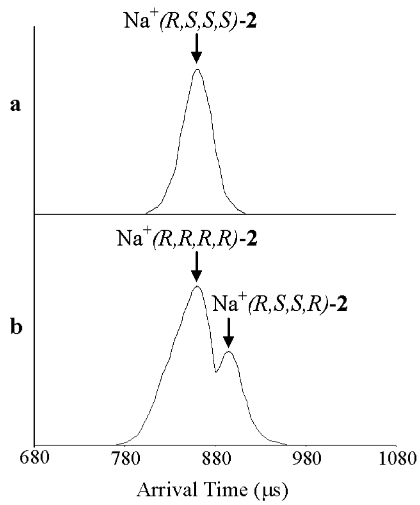

Figure 4. Arrival time distributions of (a) Na$^+$ epoxidized *meso*-**1** and (b) Na$^+$ epoxidized *rac*-**1** taken at 300 K. The peak positions of Na$^+$(*R*,*S*,*S*,*S*)-**2**, Na$^+$(*R*,*S*,*S*,*R*)-**2**, and Na$^+$(*R*,*R*,*R*,*R*)-**2** are marked above the ATDs (the enantiomer of each molecule occurs at the same arrival time).

(*S*,*R*,*R*,*S*)-**2**; approach from the open face provides (*R*,*R*,*R*,*R*)-**2** and (*S*,*S*,*S*,*S*)-**2**. If a cross-section difference of 4% occurs between (*R*,*S*,*S*,*R*)-**2** and (*R*,*R*,*R*,*R*)-**2**, two peaks would be expected in the ATD for epoxidized *rac*-**1**, while only one peak would be expected from *meso*-**1**.

Epoxidation of **1** was achieved with *meta*-chloro-peroxybenzoic acid (MCPBA) in CH_2Cl_2 at 25 °C. The starting materials were ~98% pure *meso*-**1** and *rac*-**1**. The ATDs are shown in Figure 4 for (a) Na$^+$ epoxidized *meso*-**1** and (b) Na$^+$ epoxidized *rac*-**1**. A single peak is observed in Figure 4a, corresponding to a cross section of 139 ± 2 Å^2, whereas two peaks, in a 13:7 ratio, are observed in Figure 4b, with cross sections of 140 ± 2 and 145 ± 2 Å^2.

Representations of the lowest energy family of structures for one of each unique enantiomeric pair are shown in Figure 5. For Na$^+$-(*R*,*R*,*R*,*S*)-**2**, the molecule adopts a twisted up/up configuration where one pCp core is positioned perpendicular to the other pCp core to minimize interactions with the epoxide. In this configuration, the sodium ion "binds" the oxygen and one of the two pCp faces, resulting in an average cross section of 140 ± 2 Å^2. This cross section agrees with the experimental value obtained from Figure 4a. Na$^+$(*R*,*R*,*R*,*R*)-**2** is similar to Na$^+$(*R*,*R*,*R*,*S*)-**2**, as it also orients

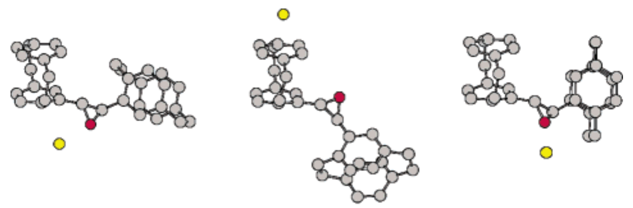

Na+(R,R,R,S)-2 Na+(R,S,S,R)-2 Na+(R,R,R,R)-2

Figure 5. Calculated structures of Na$^+$(*R*,*R*,*R*,*S*)-**2**, Na$^+$(*R*,*S*,*S*,*R*)-**2**, and Na$^+$(*R*,*R*,*R*,*R*)-**2**. C atoms are gray, O atoms are red, and Na atoms are yellow. H atoms are omitted for clarity.

itself in a twisted up/up configuration; however, the sodium ion only coordinates to the oxygen atom. The average cross section of this conformation (140 $\pm$ 2 Å^2) is in excellent agreement with the most intense peak at the shortest arrival time in Figure 4b. A twisted up/down configuration is calculated for Na$^+$(*R*,*S*,*S*,*R*)-**2**, where the sodium ion coordinates to a pCp face. The resulting average cross section for this conformation is 145 $\pm$ 2 Å^2, which agrees with the longest time peak in Figure 4b. By matching the ATD peaks with the corresponding structures for Na$^+$ epoxidized *rac*-**1**, it was confirmed that epoxidation occurs preferentially at the more open face.

In summary, we have shown that the combination of ion mobility mass spectrometry and molecular mechanics calculations provides a powerful method for diastereomer determination. This method proves useful for determining isomeric abundances in systems with different collision cross sections, and in the case of **1** and **2**, it provides for a straightforward assignment. The effect of the spatial distributions on the optoelectronic coupling in *rac*-**1** and *meso*-**1**, and its relevance to the electronic delocalization in pCp-containing conjugated polymers,[17] are the subjects of ongoing studies.

Acknowledgment. This work was funded by AFOSR (F49620-03-1-0046), ONR (N0014-9-1-0759), and NSF (DMR-0097611).

Supporting Information Available: Synthetic details. This material is available free of charge via the Internet at http://pubs.acs.org.

References

(1) Eliel, E. L.; Wilen, S. H. *Stereochemistry of Organic Compounds*; John Wiley & Sons: New York, 1994.

(2) (a) Hegstrom, R. A.; Kondepudi, D. K. *Sci. Am.* **1990**, *262*, 108. (b) Ramsay, O. B. *Stereochemistry*; Heyden and Son: Philadelphia, PA, 1981.

(3) (a) Bartholomew, G. P.; Bazan, G. C. *Acc. Chem. Res.* **2001**, *34*, 30. (b) Oldham, W. J.; Miao, Y.-J.; Lachicotte, R. J.; Bazan, G. C. *J. Am. Chem. Soc.* **1998**, *120*, 419. (c) Bazan, G. C.; Oldham, W. J.; Lachicotte, R. J.; Tretiak, S.; Chernyak, V.; Mukamel, S. *J. Am. Chem. Soc.* **1998**, *120*, 9188. (d) Wang, S.; Bazan, G. C.; Tretiak, S.; Mukamel, S. *J. Am. Chem. Soc.* **2000**, *122*, 1289. (e) Zyss, J.; Ledoux, I.; Volkov, S.; Chernyak, V.; Mukamel, S.; Bartholomew, G. P.; Bazan, G. C. *J. Am. Chem. Soc.* **2000**, *122*, 11956. (f) Bartholomew, G. P.; Ledoux, I.; Mukamel, S.; Bazan, G. C.; Zyss, J. *J. Am. Chem. Soc.* **2002**, *124*, 13480.

(4) Formal planar chirality is designated p*R* and p*S*; however, for simplicity it is referred to herein as *R* and *S*. For a description of planar chirality, see: Eliel, E. L.; Wilen, S. H. Chirality in Molecules Devoid of Chiral Centers. *Stereochemistry of Organic Compounds*; John Wiley & Sons: New York, 1994.

(5) Meso and racemic [2.2]-paracyclophane dimers have been discussed previously, see: (a) Kus, P. *Pol. J. Chem.* **1994**, *68*, 1983. (b) Jones, P. G.; Kus, P. *Pol. J. Chem.* **1998**, *72*, 1106. (c) Ernst, L.; Wittowski, L. *Eur. J. Org. Chem.* **1999**, *7*, 1653. (d) Jones, P. G.; Ernst, L.; Dix, I.; Wittowski, L. *Acta Crystallogr.* **1997**, *C53*, 612. (e) Jones, P. G.; Ernst, L.; Dix, I.; Wittowski, L. *Acta Crystallogr.* **2000**, *C56*, 239.

(6) Scholl, M.; Ding, S.; Lee, C. W.; Grubbs, R. H. *Org. Lett.* **1999**, *1*, 953.

(7) Heck, R. F. *Palladium Reagents in Organic Syntheses*; Academic Press: London, 1985.

(8) Bowers, M. T.; Kemper, P. R.; vonHelden, G.; vanKoppen, P. A. M. *Science* **1993**, *260*, 1446.

(9) Clemmer, D. E.; Jarrold, M. F. *J. Mass Spectrom.* **1997**, *32*, 577.

(10) Baker, E. S.; Gidden, J.; Fee, D. P.; Kemper, P. R.; Anderson, S. E.; Bowers, M. T. *Int. J. Mass Spectrom.* **2003**, *227*, 205.

(11) Mason, E. A.; McDaniel, E. W. *Transport Properties of Ions in Gases*; Wiley: New York, 1988.

(12) vonHelden, G.; Hsu, M. T.; Gotts, N.; Bowers, M. T. *J. Phys. Chem.* **1993**, *97*, 8182.

(13) Gidden, J.; Wyttenbach, T.; Batka, J. J.; Weis, P.; Bowers, M. T.; Jackson, A. T.; Scrivens, J. H. *J. Am. Soc. Mass Spectrom.* **1999**, *10*, 883.

(14) Gidden, J.; Bushnell, J. E.; Bowers, M. T. *J. Am. Chem. Soc.* **2001**, *123*, 5610.

(15) Case, D. A.; Pearlman, D. A.; Caldwell, J. W.; Cheatham, T. E., III; Ross, W. S.; Simmerling, C. L.; Darden, T. A.; Merz, K. M.; Stanton, R. V.; Cheng, A. L.; Vincent, J. J.; Crowley, M.; Tsui, V.; Radner, R. J.; Duan, Y.; Pitera, J.; Massova, I.; Seibel, G. L.; Sing, U. C.; Weiner, P. K.; Kollman, P. A. *AMBER 6.0*; University of California, San Francisco, 1999.

(16) Wyttenbach, T.: vonHelden, G.; Batka, J. J., Jr.; Carlat, D.; Bowers, M. T. *J. Am. Soc. Mass Spectrom.* **1997**, *8*, 275.

(17) (a) Morisaki, Y.; Chujo, Y. *Chem. Lett.* **2002**, *2*, 194. (b) Morisaki, Y.; Chujo, Y. *Macromolecules* **2002**, *35*, 587. (c) Morisaki, Y.; Ishida, T.; Chujo, Y. *Macromolecules* **2002**, *35*, 7872. (d) Morisaki, Y.; Chujo, Y. *Polym. Bull.* **2002**, *49*, 209. (e) Salhi, F.; Collard, D. *Adv. Mater.* **2003**, *15*, 81.

JA039486K